Plastic response and correlations in athermally sheared amorphous solids

F. Puosi,[1,2,*] J. Rottler,[3,†] and J-L. Barrat[1,2,4,‡]
[1]*Université Grenoble Alpes, LIPHY, F-38000 Grenoble, France*
[2]*CNRS, LIPHY, F-38000 Grenoble, France*
[3]*Department of Physics and Astronomy, The University of British Columbia, 6224 Agricultural Road, Vancouver, British Columbia V6T 1Z1, Canada*
[4]*Institut Laue-Langevin, 6 rue Jules Horowitz, BP 156, F-38042 Grenoble, France*
(Received 24 June 2016; published 21 September 2016)

The onset of irreversible deformation in low-temperature amorphous solids is due to the accumulation of elementary events, consisting of spatially and temporally localized atomic rearrangements involving only a few tens of atoms. Recently, numerical and experimental work addressed the issue of spatiotemporal correlations between these plastic events. Here, we provide further insight into these correlations by investigating, via molecular dynamics (MD) simulations, the plastic response of a two-dimensional amorphous solid to artificially triggered local shear transformations. We show that while the plastic response is virtually absent in as-quenched configurations, it becomes apparent if a shear strain was previously imposed on the system. Plastic response has a fourfold symmetry, which is characteristic of the shear stress redistribution following the local transformation. At high shear rate we report evidence for a fluctuation-dissipation relation, connecting plastic response and correlation, which seems to break down if lower shear rates are considered.

DOI: 10.1103/PhysRevE.94.032604

I. INTRODUCTION

Heterogeneity is a crucial aspect of the flow of amorphous materials. If these materials are driven by an external shear, one observes localized particle rearrangements, called shear transformations (STs), taking place in a small region while the rest of the system deforms elastically [1–3]. The effect of a shear transformation, i.e., the stress redistribution in the surrounding medium, is usually described via an elastic propagator $\mathcal{G}$, which is the solution of the Eshelby inclusion problem in a uniform elastic medium [4]. In two dimensions, $\mathcal{G}$ has a quadrupolar symmetry and it decays as r^{-2} in space. The elastic propagator is the key ingredient of rheological models for the flow of amorphous materials [5–10].

In a recent paper [11], we addressed via computer simulations of a model amorphous solid the question of the *elastic* response of an amorphous solid to localized shear transformations. We showed that the Eshelby description holds on average while for individual plastic events the response is blurred by strong fluctuations, presumably associated with the elastic heterogeneity of the material. In order to capture these fluctuations within coarse-grained rheological models, it is necessary to go beyond the equilibrium-based description of the elastic propagator [12].

Here, we extend our previous results and investigate *plastic* effects due to STs in amorphous solids. The question we want to address is to what extent a ST is able to induce subsequent plastic events in the surrounding regions. This goes back to the topic of plastic correlations, namely how a plastic event is influenced by the position of the events that occurred in the past. Plastic correlations have the strong potential to provide information about the dynamical organization of the plastic flow. This possibility motivated recent work on this topic. In athermal quasistatic simulations, Maloney and Lemaître showed that elementary events tend to organize into correlated avalanches [13]. Later, evidence for a correlation in the nonaffine displacements of a colloidal glass was first reported by Chikkadi and coworkers in experiments [14] and then confirmed by Mandal and Varnik [15,16] in numerical simulations. In Ref. [17], correlations of the local strain field were found to emerge at the transition between the Newtonian and shear-thinning regime in a flowing liquids. Similarly, in Ref. [18], the authors reported correlated plastic events in a simulation of a concentrated emulsion. Recently, some of us showed how a simple coarse-grained model is able to reproduce, with some small quantitative discrepancies, the spatiotemporal correlations between plastic events in the flow of a disordered athermal solid [19].

In this work, we will propose a detailed description of the plastic response on the particle scale by inducing artificial shear transformations in the system and observing their response in time, and compare with previous results for their correlations. Such a characterization is particularly relevant in view of the development of realistic models for the flow of amorphous solids, especially those belonging to the family of so-called elastoplastic models [5–10]. The very point of these models is to describe precisely non-mean-field effects. Therefore, the study of plastic correlations represents a powerful tool for comparison between different models and between models and experiments in systems in which the corresponding observables are experimentally accessible.

The paper is organized as follows. Details about the model and the procedure to simulate artificial shear transformations are given in Sec. II. Results of the numerical simulations are discussed in Sec. III, while Sec. IV provides a short summary and discussion.

*francesco.puosi@univ-grenoble-alpes.fr
†jrottler@phas.ubc.ca
‡jean-louis.barrat@univ-grenoble-alpes.fr

II. MODEL AND DETAILS OF THE SIMULATION

We consider a generic two-dimensional (2D) model of a glass, consisting of a mixture of A and B particles, with $N_A = 32\,500$ and $N_B = 17\,500$, interacting via a Lennard-Jones potential $V_{\alpha\beta}(r) = 4\epsilon_{\alpha\beta}[(\frac{\sigma_{\alpha\beta}}{r})^{12} - (\frac{\sigma_{\alpha\beta}}{r})^{6}]$ with $\alpha,\beta = A,B$ and r being the distance between two particles. The parameters ϵ_{AA}, σ_{AA}, and m_A define the units of energy, length, and mass; the unit of time is given by $\tau_0 = \sigma_{AA}\sqrt{(m_A/\epsilon_{AA})}$. We set $\epsilon_{AA} = 1.0$, $\epsilon_{AB} = 1.5$, $\epsilon_{BB} = 0.5$, $\sigma_{AA} = 1.0$, $\sigma_{AB} = 0.8$, $\sigma_{BB} = 0.88$, and $m_A = m_B = 1$. With this choice, the system is stable against crystallization in two dimensions [20]. A similar system was used by Falk and Langer [2] to study plasticity in 2D metallic glasses. The potential is truncated at $r = r_c = 2.5$ for computational convenience. The simulation box dimensions $L_x = L_y = 205$ are fixed and periodic boundary conditions are used. The equations of motion are integrated using the velocity Verlet algorithm with a time step $\delta t = 0.005$. The athermal limit is achieved by thermostating the system at zero temperature via a Langevin thermostat [21] with a damping coefficient $\Gamma = 1$; the associated equations of motion are

$$\frac{d\mathbf{r}_i}{dt} = \frac{\mathbf{p}_i}{m}, \tag{1}$$

$$\frac{d\mathbf{p}_i}{dt} = -\sum_{j\neq i}\frac{\partial V(\mathbf{r}_{ij})}{\partial \mathbf{r}_{ij}} - \Gamma\mathbf{p}_i, \tag{2}$$

where $(\mathbf{p}_i,\mathbf{r}_i)$ are the momentum and the position of particle i. As $T = 0$, no fluctuating force appears in the equations.

Glassy states were prepared by quenching equilibrated systems at $T = 1$ to zero temperature with a fast rate $dT/dt = 2\times10^{-3}$ while maintaining constant volume. Simple shear is imposed at a rate $\dot\gamma$ by deforming the box dimensions and remapping the particles positions. For the present model the yield strain, defined as the strain at the maximum stress in the stress-strain curve, is approximately 8–9%. Local shear transformations (STs) are generated by applying a pure shear strain ϵ to a circular region of radius $a = 2.5$ centered at (x_0,y_0), as discussed in Ref. [11]. Particles inside the region, at the initial position (x_i,y_i), are displaced to (x_i',y_i') according to

$$\begin{aligned} x_i &\to x_i' = x_i + \epsilon(y_i - y_0),\\ y_i &\to y_i' = y_i + \epsilon(x_i - x_0). \end{aligned} \tag{3}$$

The transformation is instantaneous and sets the time origin $t = 0$. The positions of the particles in the ST are frozen and the behavior of the surrounding ones at later times is observed. For as-quenched configurations, the response is averaged over 10 independent realizations and for each of those 50 positions for the ST center (x_0,y_0) are considered. For presheared configurations, we average the response over independent realizations (4 starting configurations), strain (16 strain values in the range $0.2 \leqslant \gamma \leqslant 1.0$), and position of the ST center (20 position), resulting in an average over 1280 trajectories.

Plastic activity is described by the $D^2_{\min}$ quantity introduced by Falk and Langer [2], which evaluates deviations from an affine deformation on a local scale. For a given particle i, $D^2_{\min}$ is defined as the minimum over all possible linear deformation tensors $\epsilon_{\rm loc}$ of

$$D^2(i,t_0,t) = \sum_j [r_{ij}(t_0+t) - (\mathbb{I} + \epsilon_{\rm loc})r_{ij}(t_0)]^2, \tag{4}$$

where the index j runs over all the neighbors of the reference particle i and $\mathbb{I}$ is the identity matrix.

III. RESULTS AND DISCUSSION

A. As-quenched configurations

In Ref. [11], the local strain ϵ was set to a few percent ($\epsilon = 0.025$) in order to probe the elastic reversible response of the system to STs. Here, we investigate the effects of a higher local strain in amorphous configurations at $T = 0$, rapidly quenched from high temperature. We define the plastic response function,

$$R_2(\mathbf{r},\Delta t) = \overline{D^2}_{\min}(\mathbf{r},t_0,t_0+\Delta t)/(a^2\epsilon^2), \tag{5}$$

where $\overline{D^2}_{\min}$ is the coarse-grained $D^2_{\min}$-field obtained by mapping particles into a grid with a spacing $\xi = 1$, t_0 is the time at which the ST is applied, and a and ϵ are the radius and local strain of the ST, respectively. In Fig. 1 spatial maps of $R_2(\mathbf{r},\Delta t)$ for $\Delta t = 10^3$, which corresponds to the long time limit, are shown for larger values of the applied strain. We observe that the plastic activity is very weak, being restricted to a small region close to the ST center, and that it does not depend on the specific value of the strain ϵ. Even for a strain of 10%, the response is almost entirely elastic.

B. Sheared configurations

We now focus on the effects of external deformation on the tendency of the system to undergo plastic rearrangements. Simple shear is imposed on the system at a rate $\dot\gamma$ before applying the shear transformation protocol. Steady-state configurations with a strain $\gamma \geqslant 0.2$ are considered as starting configurations. Then the accumulated stress is not relaxed and the strain γ is kept constant in the following temporal evolution, specifically $\dot\gamma$ is instantaneously set to zero. The time evolution of the plastic response in sheared configurations is shown in Fig. 2 for three distinct shear rates $\dot\gamma = 10^{-6}$,

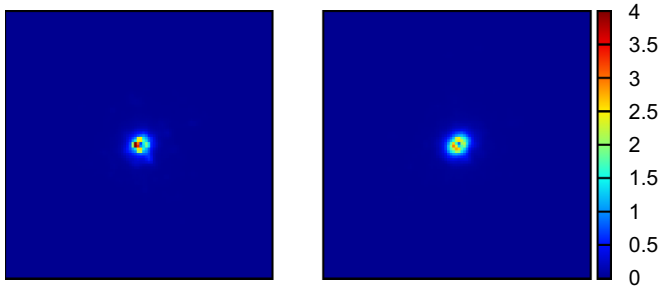

FIG. 1. Plastic response field $R_2(\mathbf{r},\Delta t)$, as defined in Eq. (5), induced by a shear transformation (at the center of the cell) in the long time limit $\Delta t = 10^3$ for as-quenched configurations. Data for two different values of the shear strain ϵ are shown: 0.05 (left) and 0.1 (right). A region of size 200×200 around the ST is shown and the color corresponds to the amplitude of the plastic response field.

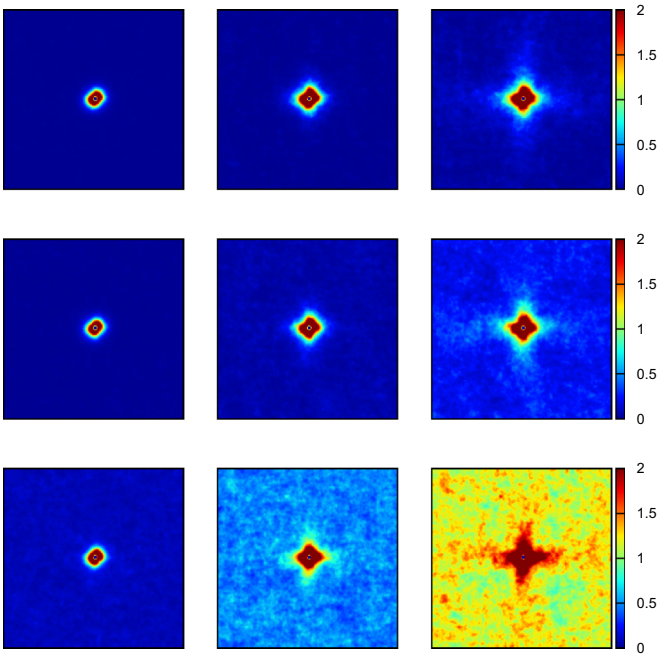

FIG. 2. Plastic response field $R_2(\mathbf{r},\Delta t)$, as defined in Eq. (5), induced by a ST in sheared configurations for different time lags Δt. Data are shown for different shear rates $\dot\gamma = 10^{-6}$ (top), $\dot\gamma = 10^{-5}$ (middle), and $\dot\gamma = 10^{-4}$ (bottom) and for different time lags $\Delta t = 4$ (left column), $\Delta t = 20$ (central column) and $\Delta t = 100$ (right column). A region of size 200×200 around the ST is shown.

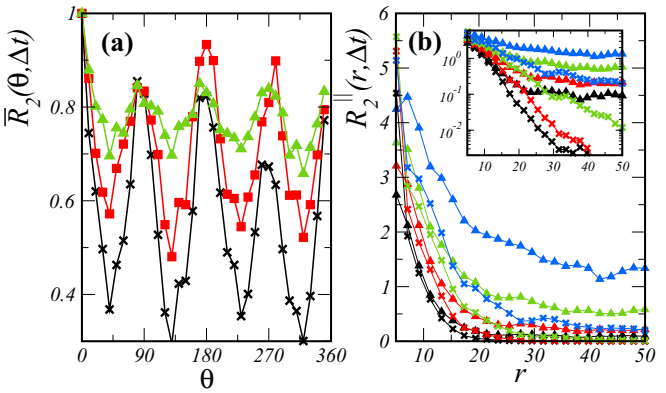

FIG. 3. (a) Angular dependence of the plastic response $\overline{R}_2(\theta,\Delta t) = \alpha \int_{2a}^{L/2} R_2(r,\theta,\Delta t)dr$ (see text). Data are shown for $\Delta t = 100$ and for different shear rates $\dot\gamma = 10^{-4}$ (triangles), $\dot\gamma = 10^{-5}$ (squares), and $\dot\gamma = 10^{-6}$ (crosses). (b) Plastic response along the shear direction $R_2^{\parallel}$ in lin-lin (main panel) and lin-log (inset) plots. Data are shown for different time lags $\Delta t = 4$ (black), $\Delta t = 8$ (red), $\Delta t = 20$ (green), and $\Delta t = 40$ (blue), and for different shear rates $\dot\gamma = 10^{-4}$ (triangles) and $\dot\gamma = 10^{-6}$ (crosses).

10^{-5}, and 10^{-4}. First, with respect to the case of as-quenched systems, the effect of the preshearing is apparent in the increased plastic activity even for short time lags. Looking at long times, the pattern of the plastic activity clearly resembles the elastic propagator $\mathcal{G} \sim \cos(4\theta)/r^2$, which controls the stress redistribution following the ST. High plastic intensity is observed in the streamwise ($\theta = 0^\circ$) and crosswise ($\theta = 90^\circ$) directions, which correspond to the directions of positive stress release. On the other hand, the redistributed stress is negative along the diagonal and this results in lower plastic activity. It is straightforward to rationalize these observations: in the presheared configurations, many regions have already been loaded close to the yield point, and the stress redistribution following the primary ST can trigger plastic events much more easily than starting from as-quenched configurations.

This picture becomes clearer if one considers the angular dependence of the plastic response, as denoted by the quantity $\overline{R}_2(\theta,\Delta t) = \alpha \int_{2a}^{L/2} R_2(r,\theta,\Delta t)dr$, where L is the system size and the prefactor α is chosen such that $\overline{R}_2(\theta,\Delta t)$ has a maximum of 1. The long time limit of $\overline{R}_2(\theta,\Delta t)$ is shown in Fig. 3(a) for different shear rates. We observe again the quadrupolar modulation characteristic of the Eshelby response function, which becomes more pronounced with decreasing shear rate. Here we point out that no clear asymmetry is observed between streamwise and crosswise lobes, in contrast with previous results on plastic correlations [19], where streamwise peaks appeared to be stronger than crosswise ones at low shear rates. However, we cannot exclude that in our case this effect is still hidden by the noise. Figures 2 and 3 also show that as $\dot\gamma$ increases a plastic background emerges. This is due to a cascade effect, with the primary ST triggering plastic rearrangements, which themselves play the role of sources for subsequent events. This phenomenon is more prevalent at higher driving rates.

In Fig. 3(b) we show the spatial decay of the response function along the shear direction $R_2^{\parallel}$ at different times and for different shear rates. The response extends to larger distances as the time interval increases, consistent with the propagation of the strain field created by the ST, as discussed previously [11]. The decay of $R_2^{\parallel}$ is approximately exponential (see the inset of the figure). This observation agrees with previous results for the correlations of plasticity in models of amorphous systems [16,19,22]. In fact, in Ref. [16] the authors argue that the spatial decay of the $D^2_{\min}$ correlations is dependent on the specific implementation of the dissipation scheme in the equations of motion: friction based on the relative velocity of a particle with respect to its neighbors results in a power-law decay, whereas a "mean-field" dissipation scheme, such as the one used in the present work, results in an exponential decay. Further, the response seems to be independent on the shear rate: at short times, data for the different shear rates are indistinguishable, whereas deviations are observed at larger times due to the emerging background plasticity mentioned before.

In order to confirm the proposed scenario of a plastic response controlled by the Eshelby elastic propagator, we investigate the response to a ST whose principal axes are rotated by an angle $\phi = 90^\circ$ with respect of the shear direction. This rotation of the local strain matrix is equivalent to a sign change in ϵ. According to the quadrupolar symmetry of the propagator, this should result in a rotation of the response pattern by 45° with respect to the one observed for $\phi = 0^\circ$ discussed above. In Fig. 4 we show the response to the rotated ST. If we focus on the angular dependence Fig. 4(a), we observe that the main peaks are shifted by 45°, as expected.

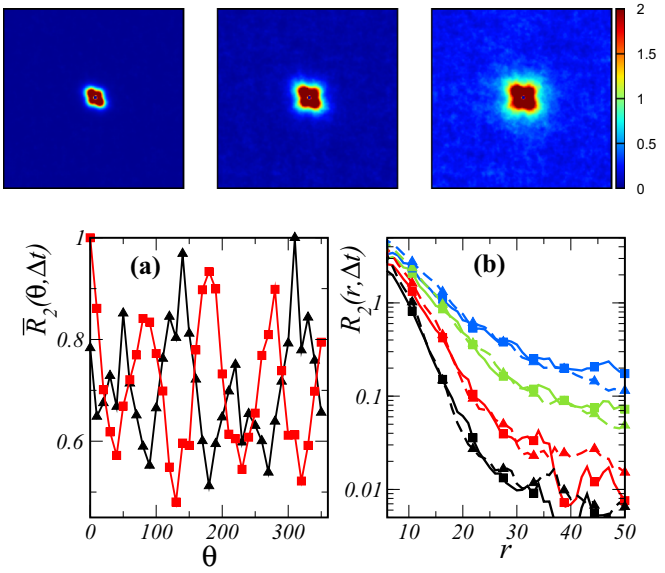

FIG. 4. Top: plastic response field $R_2(\mathbf{r},\Delta t)$ at different time lags, $\Delta t = 4$ (left), $\Delta t = 4$ (center), and $\Delta t = 100$ (right), induced by a ST whose main axis is rotated by an angle $\phi = 90^\circ$ with respect to the shear direction ($\dot\gamma = 10^{-5}$). Bottom, panel (a), corresponding angular dependence for $\Delta t = 100$ (triangles); for comparison, data for $\phi = 0^\circ$ are also shown (squares). Bottom, panel (b), spatial decay along a principal direction θ^* at different time lags, $\Delta t = 4$ (black), $\Delta t = 8$ (red), $\Delta t = 20$ (green), and $\Delta t = 40$ (blue), for $\phi = 90^\circ$ with $\theta^* = 45^\circ$ (triangles) and the reference $\phi = 0^\circ$ with $\theta^* = 0^\circ$ (squares).

Further, as shown in Fig. 4(b), the spatial decay of the response at different time lags along the principal direction $\theta^* = 45^\circ$ is in very good agreement with that for the unrotated case where the shear direction is $\theta^* = 0^\circ$.

C. Response and correlation

We now turn to a quantitative comparison between plastic response and correlations. In Ref. [19], some of us presented for the same model amorphous solid a detailed description of the plastic events and their dynamical correlations, resolved both in space and time, using the two-point, two-time plastic correlator,

$$C_2(r,\Delta t) = \alpha\Big(\big\langle\overline{D^2_{\min}(r_0,t_0)D^2_{\min}(r_0+r,t_0+\Delta t)}\big\rangle - \big\langle\overline{D^2_{\min}(r_0,t_0)D^2_{\min}(r_0,t_0+\Delta t)}\big\rangle\Big), \quad (6)$$

where the brackets denote an average over time t_0, the bars represent an average over spatial coordinate r_0, and the prefactor α is chosen such that $C_2(r=0,\Delta t=0)=1$. C_2 measures the (enhanced or reduced) likelihood that a plastic event occurs at $r_0 + r$ if a plastic event was active at position r_0 some prescribed time Δt ago.

In the first instance, one could imagine comparing directly the correlation C_2 to the response function R_2. In this case, the two quantities show strongly different behavior with the correlation extending to larger distances with respect to response for equal time lags (not shown). However, we argue that this is not the most significant comparison. Indeed, assuming a linear response perspective, with the strain ϵ of the ST acting as perturbation, the most appropriate quantity to focus on seems to be $(D^2_{\min})^{1/2}$ rather than $D^2_{\min}$ ($D^2_{\min}$ is a squared displacement, which depends quadratically on the local strain tensor $\epsilon_{\rm loc}$). In this spirit, we define the response function $R_1(r,\Delta t)$,

$$R_1(r,\Delta t) = \big(R_2(r,\Delta t) - R_2^\infty(\Delta t)\big)^{1/2}, \quad (7)$$

and the corresponding correlation function $C_1(r,\Delta t)$,

$$C_1(r,\Delta t) = \alpha\Big(\big\langle\overline{\big(D^2_{\min}(r_0,t_0)\big)^{1/2}\big(D^2_{\min}(r_0+r,t_0+\Delta t)\big)^{1/2}}\big\rangle - \big\langle\overline{\big(D^2_{\min}(r_0,t_0)\big)^{1/2}\big(D^2_{\min}(r_0,t_0+\Delta t)\big)^{1/2}}\big\rangle\Big), \quad (8)$$

where in Eq. (7) the background response $R_2^\infty(\Delta t)$ is subtracted.

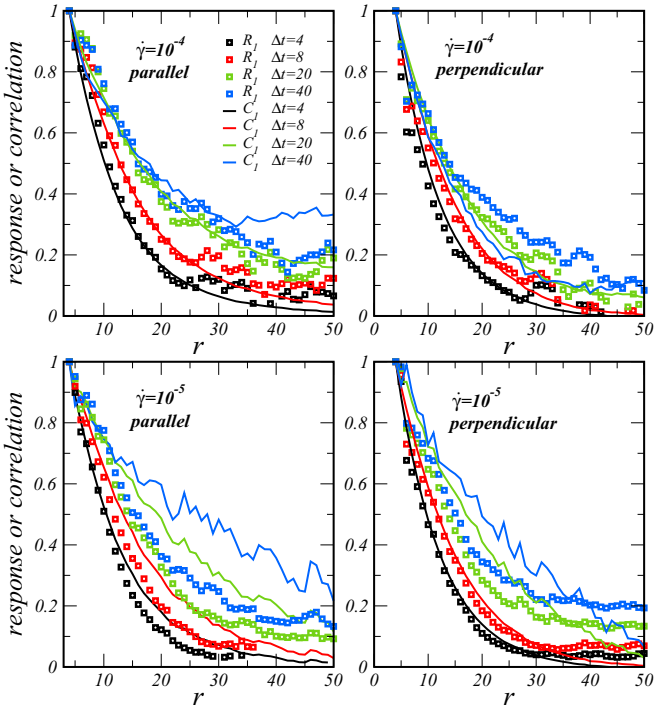

FIG. 5. Decay of the plastic response $R_1(r,\Delta t)$ (symbols) and correlation $C_1(r,\Delta t)$ (lines) in the direction parallel and perpendicular to the shear direction. Data are shown for different shear rates $\dot\gamma = 10^{-4}$ (top panels), $\dot\gamma = 10^{-5}$ (bottom panels), and for different time lags $\Delta t = 4$ (black), $\Delta t = 8$ (red), $\Delta t = 20$ (green), and $\Delta t = 40$ (blue). Data are vertically rescaled in order to have $R_1(r,\Delta t) = C_1(r,\Delta t) = 1$ at $r = 4$. The relative distance between R_1 and C_1 can be defined as $\Delta_1(\Delta t) = \int_{2a}^{L/4} |R_1(r,\Delta t) - \beta C_1(r,\Delta t)|dr / \int_{2a}^{L/4} |R_1(r,\Delta t)|dr$, where the integral is calculated along a given direction (parallel or perpendicular to the flow). We note that Δ_1 is smaller than 0.2 for all directions at large strain rate $\dot\gamma = 10^{-4}$ and larger for the small one $\dot\gamma = 10^{-5}$.

In Fig. 5, we compare the decay of the response and correlation functions $R_1(r,\Delta t)$ and $C_1(r,\Delta t)$ along the directions parallel and perpendicular to the shear direction. First, we focus on the high shear rate $\dot\gamma = 10^{-4}$. Here, we observe that the decay of the response strongly resembles that of the correlation showing an almost exponential decay with a comparable extension. This applies both to the parallel and perpendicular directions. By contrast, for the low shear rate $\dot\gamma = 10^{-5}$ differences become apparent, with the correlation

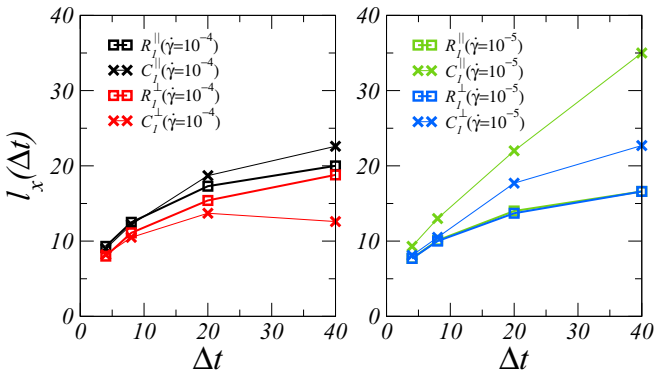

FIG. 6. Time dependence of the decay length l for the plastic response (open squares) and correlation (crosses). Data are shown for the directions parallel and perpendicular to the shear direction and for different shear rates.

extending to larger distances. Deviations are stronger in the shear direction, especially for large time lags, whereas they are weaker in the perpendicular direction.

Assuming purely exponential behavior $x(r,\Delta t) = A_x(r,\Delta t)\exp(-r/l_x(\Delta t))$ with $x = R_1, C_1$, we can estimate the decay length $l_x(\Delta t)$. In Fig. 6 we show the time dependence of the decay length for response and correlation in the two directions and for different shear rates. For the highest shear rate $\dot\gamma = 10^{-4}$, l_{R_1} and l_{C_1} grow with time approximately in the same way, $l_x(\Delta t) \sim t^{\kappa}$ with an exponent $\kappa \approx 0.5$, suggesting diffusive spreading for both the response and the correlation. Conversely, for the lower rate $\dot\gamma = 10^{-5}$, whereas for the response the growth is still sublinear, it is faster for the correlation, with the effect being stronger along the parallel direction, where an almost linear behavior is observed.

At this point, it is quite natural to interpret the results concerning correlation and response in the framework of the fluctuation-dissipation theorem. We briefly recall here that for a system at equilibrium, a response function $R(t)$ and the associated correlation function $C(t)$ are related by a fluctuation-dissipation relation (FDR) $R(t) = -(k_B T)^{-1}\partial_t C(t)$. This relation has to be generalized in out-of-equilibrium systems by introducing an effective temperature $T_{\rm eff}$, which replaces the bath temperature T [23,24]. Our results would suggest for the high shear rate $\dot\gamma = 10^{-4}$ the existence of a FDR of the form $R_1(r,\Delta t) = \beta C_1(r,\Delta t)$ with β carrying information about an effective temperature, $\beta \sim 1/T_{\rm eff}$. If we restrict ourselves to short time lags $\Delta t \leqslant 20$, we estimate $\beta \sim 2.8$ for the parallel direction and $\beta \lesssim 2.0$ for the perpendicular one. We note that, since we have no further information about the appropriate prefactors, we are unable to extract from β any absolute value for the effective temperature. The scenario is different for the lower rate $\dot\gamma = 10^{-5}$ where response and correlation deviate more strongly and no FDR seems to hold.

We note here that there is no theoretical justification in our system for looking *a priori* for a response-correlation proportionality, as the shear transformation is a strongly nonlinear local perturbation, as is the response in the form of a plastic activity. However, at a coarse-grained level, and in the spirit of elasto plastic models, the shear transformation can be considered as the elementary "dynamical event" that governs the dynamics. As a result, it is natural to investigate the similarity between the response to a triggered shear transformation (response function) and the response to one that is taking place spontaneously (correlation function). In a system at thermal equilibrium responding to a small perturbation, these two quantities are proportional, and the system does not distinguish between the external perturbation and spontaneous fluctuations. Observing a similar property at the level of the local strain would imply that the driven system is brought, at the level of this variable, into a state that resembles thermodynamic equilibrium at a finite temperature.

IV. CONCLUSION

This work represents an extension of a previous study [11], where we have investigated the response of a standard 2D model glass to artificially triggered local shear transformations, which replicates elementary plastic events observed in amorphous solids under deformation. No significant plastic response is observed in as-quenched configurations, even for very large strains applied to the ST. By contrast, presheared configurations exhibit long-ranged response behavior with quadrupolar symmetry.

We have also compared quantitatively the spatiotemporal decay of the response functions to correlations between plastic events measured in the same model system during steady flow. At the highest rate considered here, correlations and response appear to be proportional to each other, suggesting the existence of a nonequilibrium generalization of the fluctuation-dissipation theorem for plastic activity. Such generalizations that imply the existence of an effective temperature have been previously reported for other observables in driven systems during steady state [25–27]. By contrast, our (limited) data at lower shear rates suggest that this behavior does not hold in general in the present system.

One could think of a few reasons for this difference. First, we note that the correlation function also includes correlated but not causally linked events that are the consequence of earlier events. Let's consider a slip line where a large event triggers two other events: the correlation function will include the correlation between these two last events, despite the fact that one is not the cause of the other. This scenario is confirmed by the observation of a nonzero correlation for a zero time lag [19]. Clearly, for the response this effect is lost since we trigger artificial events at random positions in the system. One could imagine that this noncausal correlation plays a more important role for low shear rates. In addition to this effect, which we believe to be the dominant one, other second-order issues are present. Indeed, we are looking at the strongly nonlinear response of a system that is not undergoing external driving (although the initial configuration has been prepared by an external drive), whereas the correlation clearly refers to a driven system in steady state. However, we find (not shown) that keeping the external drive while triggering the zone does not affect the system response. This is not surprising since we are dealing with relatively short time lags. Moreover, any effect due to stopping the driving would be present, and probably stronger, also for the highest rate, but this seems not to be the case.

An additional possible source of discrepancy could lie in the fact that the triggered STs are instantaneous, while the spontaneous plastic events have a finite duration. From previous simulation results [19], the typical timescale of a plastic events is of the order of a few time units, which is not very well separated from the time window of the response. We expect that including a finite duration in the triggering protocol would have the effect of slowing down the response propagation, thus increasing the discrepancies with the correlation.

Finally, the last possibility that comes to our mind is that the system around a soft spot, at which the spontaneous shear transformation is taking place, is somehow organized in a rather different manner than around the random places we are choosing to trigger the artificial transformations. This idea is consistent with the fact that FDR-like behavior is emerging at the highest driving rate, where correlations between plastic events and soft spots are reduced [28] and would deserve further attention in future work.

ACKNOWLEDGMENTS

The simulations were carried out using LAMMPS molecular dynamics software [29,30]. J.L.B. and F.P. are supported by Institut Universitaire de France and by Grant No. ERC-2011-ADG20110209. All the computations presented in this paper were performed using the Froggy platform of the CIMENT infrastructure [31], which is supported by the Rhône-Alpes region (Grant No. CPER07_13 CIRA) and the Equip@Meso project (Grant No. ANR-10-EQPX-29-01) of the programme Investissements d'Avenir supervised by the Agence Nationale pour la Recherche. We thank Alexandre Nicolas for fruitful discussions.

[1] A. Argon and H. Kuo, Mater. Sci. Eng. **39**, 101 (1979).
[2] M. L. Falk and J. S. Langer, Phys. Rev. E **57**, 7192 (1998).
[3] P. Schall, D. A. Weitz, and F. Spaepen, Science **318**, 1895 (2007).
[4] J. D. Eshelby, Proc. R. Soc. London A **241**, 376 (1957).
[5] G. Picard, A. Ajdari, F. Lequeux, and L. Bocquet, Eur. Phys. J. E **15**, 371 (2004).
[6] G. Picard, A. Ajdari, F. Lequeux, and L. Bocquet, Phys. Rev. E **71**, 010501 (2005).
[7] D. Vandembroucq and S. Roux, Phys. Rev. B **84**, 134210 (2011).
[8] K. Martens, L. Bocquet, and J.-L. Barrat, Phys. Rev. Lett. **106**, 156001 (2011).
[9] K. Martens, L. Bocquet, and J.-L. Barrat, Soft Matter **8**, 4197 (2012).
[10] A. Nicolas, K. Martens, L. Bocquet, and J.-L. Barrat, Soft Matter **10**, 4648 (2014).
[11] F. Puosi, J. Rottler, and J.-L. Barrat, Phys. Rev. E **89**, 042302 (2014).
[12] A. Nicolas, F. Puosi, H. Mizuno, and J.-L. Barrat, J. Mech. Phys. Solids **78**, 333 (2015).
[13] C. Maloney and A. Lemaître, Phys. Rev. Lett. **93**, 195501 (2004).
[14] V. Chikkadi, S. Mandal, B. Nienhuis, D. Raabe, F. Varnik, and P. Schall, Europhys. Lett. **100**, 56001 (2012).
[15] S. Mandal, V. Chikkadi, B. Nienhuis, D. Raabe, P. Schall, and F. Varnik, Phys. Rev. E **88**, 022129 (2013).
[16] F. Varnik, S. Mandal, V. Chikkadi, D. Denisov, P. Olsson, D. Vågberg, D. Raabe, and P. Schall, Phys. Rev. E **89**, 040301 (2014).
[17] J. Chattoraj and A. Lemaître, Phys. Rev. Lett. **111**, 066001 (2013).
[18] R. Benzi, M. Sbragaglia, P. Perlekar, M. Bernaschi, S. Succi, and F. Toschi, Soft Matter **10**, 4615 (2014).
[19] A. Nicolas, J. Rottler, and J.-L. Barrat, Eur. Phys. J. E **37**, 50 (2014).
[20] R. Brüning, D. A. St-Onge, S. Patterson, and W. Kob, J. Phys.: Condens. Matter **21**, 035117 (2009).
[21] T. Schneider and E. Stoll, Phys. Rev. B **17**, 1302 (1978).
[22] T. Sentjabrskaja, P. Chaudhuri, M. Hermes, W. C. K. Poon, J. Horbach, S. U. Egelhaaf, and M. Laurati, Sci. Rep. **5**, 11884 (2015).
[23] L. F. Cugliandolo, J. Kurchan, and L. Peliti, Phys. Rev. E **55**, 3898 (1997).
[24] L. F. Cugliandolo, J. Phys. A: Math. Theoret. **44**, 483001 (2011).
[25] L. Berthier and J.-L. Barrat, J. Chem. Phys. **116**, 6228 (2002).
[26] C. S. O'Hern, A. J. Liu, and S. R. Nagel, Phys. Rev. Lett. **93**, 165702 (2004).
[27] T. K. Haxton and A. J. Liu, Phys. Rev. Lett. **99**, 195701 (2007).
[28] S. S. Schoenholz, A. J. Liu, R. A. Riggleman, and J. Rottler, Phys. Rev. X **4**, 031014 (2014).
[29] S. Plimpton, J. Comput. Phys. **117**, 1 (1995).
[30] http://lammps.sandia.gov.
[31] https://ciment.ujf-grenoble.fr.